

Is the HR 8799 extrasolar system destined for planetary scattering?

Krzysztof Goździewski[★] and Cezary Migaszewski[★]

Nicolaus Copernicus University, Gagarin Str. 11, 87-100 Toruń, Poland

Accepted 2009 April 16. Received 2009 April 14; in original form 2009 March 13

ABSTRACT

The recent discovery of a three-planet extrasolar system of HR 8799 by Marois et al. is a breakthrough in the field of the direct imaging. This great achievement raises questions on the formation and dynamical stability of the system, because Keplerian fits to astrometric data disrupt during ~ 0.2 Myr. We search for stable, self-consistent N -body orbits with the so-called GAMP (genetic algorithm with MEGNO penalty) method that incorporates stability constraints into the optimization algorithm. Our searches reveal only small regions of stable motions in the phase space of three-planet, coplanar configurations. Most likely, if the planetary masses are in $10 M_J$ range, they may be stable only if the planets are involved in two- or three-body mean motion resonances (MMRs). We found that 80 per cent systems found by GAMP that survived 30 Myr backwards integrations, eventually become unstable after 100 Myr. It could mean that the HR 8799 system undergo a phase of planet–planet scattering. We test a hypothesis that the less certain detection of the innermost object is due to a blending effect. In such a case, two-planet best-fitting systems are mostly stable, on quasi-circular orbits and close to the 5:2 MMR, resembling the Jupiter–Saturn pair.

Key words: methods: N -body simulations – methods: numerical – stars: individual: HR 8799.

1 INTRODUCTION

The HR 8799 planetary system was detected by Marois et al. (2008) through the direct imaging. Soon, a new observation was added by Lafrenière et al. (2009) who re-analysed images done in 1998, extending the observational window to ~ 10 yr and four different epochs. [We skip the most recent observation in Fukagawa et al. (2009) that appeared after we finished this Letter, because it did not change the initial condition.] Although the semimajor axes are large (about of 24, 36 and 68 au, respectively), the companions strongly interact mutually. As we show, their orbits remain in extremely chaotic zone spanned by low-order mean motion resonances (MMRs). We attempt to constrain the initial conditions by available astrometric data and seemingly obvious requirement of astronomical stability. Our work complements papers of Fabrycky & Murray-Clay (2008) and Reidemeister et al. (2009). Here, we follow a different approach that relies on quasi-global, self-consistent search for stable best-fitting systems, the so-called GAMP (genetic algorithm with MEGNO penalty; e.g. Goździewski, Migaszewski & Musielński 2008) which was used to model the radial velocity data. The direct imaging seems also a particularly good target for this numerical technique.

Following astrometric estimates of the semimajor axes, we see that the observational window covers a tiny part of orbital periods which are counted in hundreds of years. The initial condition may be determined with a significant error. To illustrate this uncertainty, we

map the multicube of astrometric coordinates $x(t)$, $y(t)$ and velocities $v_x(t)$, $v_y(t)$ [from the slope of $x(t)$, $y(t)$] within 3σ level of the linear model of $x(t)$, $y(t)$ on to osculating Keplerian elements at the epoch of 2008 September 18. This most reasonable choice follows the very short time-span of observations. The data set consists of 13 mean positions in $[E, N]$ -axes in Marois et al. (2008) as well as one observation in Lafrenière et al. (2009); we also adopted a standard *Hipparcos* distance to the star of 39.4 ± 1.1 pc.

The astrometric model is parametrized by the stellar mass m_0 , N tuples of Keplerian elements $\mathbf{p}_p = [m (M_J), a (\text{au}), e, \omega (^\circ), \mathcal{M}_0 (^\circ)]$, i.e. the mass, semimajor axis, eccentricity, argument of pericentre and the mean anomaly (or longitude), for each planet $p = 1, \dots, N$, respectively, and two Euler angles describing the inclination (i) and the nodal longitude (Ω) of the orbital plane with respect to the plane of the sky. The $(\chi^2_{\nu})^{1/2}$ function is build up from deviations of the astrometric measurements from coplanar, projected orbits. It depends indirectly on the astrophysical mass constraints through the transformation of the velocity–Keplerian elements. Following Marois et al. (2008) the planetary masses are $m_b = 7_{-2}^{+4} M_J$, $m_c = 10 \pm 3 M_J$, $m_d = 10 \pm 3 M_J$; the mass of the parent star is $m_0 = 1.5 \pm 0.3 M_{\odot}$. They are roughly consistent with the recent, independent estimates of Reidemeister et al. (2009). In our simulations, all masses are free parameters which are varied within their 1σ error ranges. (Moreover, a proper mass determination may be critically important for the stability analysis.) Fig. 1 shows levels of $(\chi^2_{\nu})^{1/2}$ in selected two-dimensional planes of osculating elements at the epoch of 2008 September 18. The best-fitting solution is marked with a green triangle. It is roughly consistent with a model of not too eccentric, face-on orbits by the discovery team. In fact, the limited astrometric data permit a continuum of models with different orbital

[★]E-mail: k.gozdziwski@astri.umk.pl (KG); c.migaszewski@astri.umk.pl (CM)

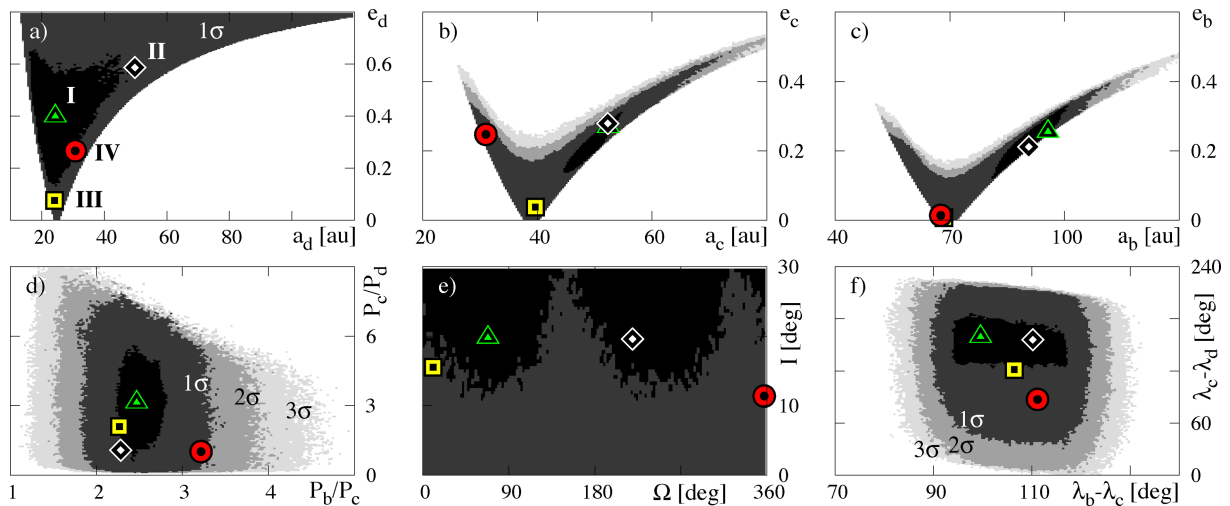


Figure 1. Global topology of $(\chi_v^2)^{1/2}$ projected on to selected planes of Keplerian, osculating elements at the epoch of 2008 September 18. Symbols are for the best-fitting systems analysed in this work. They are labelled accordingly with Table 1. Shaded areas are for 1σ , 2σ and 3σ levels labelled in panel (a, d, f) [$(\chi_v^2)^{1/2} < 1.67$, $(\chi_v^2)^{1/2} < 1.85$ and $(\chi_v^2)^{1/2} < 2.09$, respectively] of the best Fit I marked with green triangles darker shade means better fit. Black regions are for $(\chi_v^2)^{1/2}$ only marginally worse from the best-fitting value. Other fits analysed in this work are marked with white diamonds (Fit II, unstable Trojans), yellow rectangles (Fit III, the best-fitting stable configuration) and red circles (Fit IV, stable Trojans). See Fig. 2 for a geometry of these solutions.

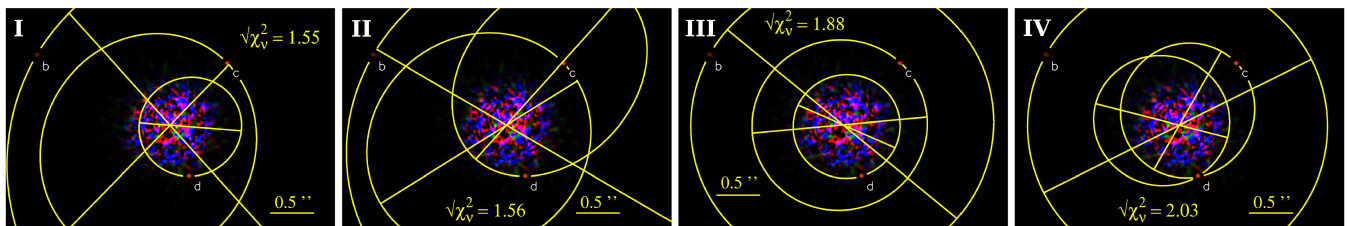


Figure 2. Orbital geometry of the best-fitting configurations projected on to the plane of the sky and the true image of the system by combined photographs taken with the Keck II adaptive optics. The planets appear as red dots around the residual scattered light of the star (seen in the centre). The best-fitting osculating orbits at the epoch of 2008 September 18 are drawn with yellow ellipses. Straight lines are for the apsidal lines of these orbits. The HR 8799 image credit: C. Marois (NRC-HIA), IDPS survey and Keck Observatory. See Table 1 for the osculating elements of these fits labelled accordingly.

characteristics, e.g. eccentricities within 1σ level of the best fit may be as large as ~ 0.4 . The orbital periods consistent with relatively small $(\chi_v^2)^{1/2}$ may be found in the proximity of numerous MMRs. In turn, these factors strongly affect the dynamical stability of the system.

The geometry of the nominal, best-fitting solution with $(\chi_v^2)^{1/2} \sim 1.55$, overplotted on the original image, is illustrated in Fig. 2(I). This best-fitting system appears strongly unstable and self-disrupts after ~ 0.2 Myr, so our conclusion is the same as in Fabrycky & Murray-Clay (2008). Moreover, according to our Fig. 1(d), very different orbital solutions are possible. For instance, two inner planets might be involved in 1c:1d MMR, or other low-order MMRs. An example of unusual Trojan configuration with only marginally worse $(\chi_v^2)^{1/2} \sim 1.56$ from the best-fitting model is shown in Fig. 2(II). Furthermore, such ‘raw’ kinematic fits are catastrophically unstable during the first Myr. Curiously, in these solutions, m_0 tends to the lowest possible limit that might indicate an internal inconsistency of the model with the data, if we recall that the stellar mass is constrained a priori.

2 THE BEST-FITTING STABLE CONFIGURATIONS

Recent works (e.g. Chatterjee et al. 2008; Jurić & Tremaine 2008; Scharf & Menou 2009, and references therein) showed that com-

pact planetary systems may evolve towards configurations spanning wide ranges of orbital elements. The long-period planets could place constraints on early stage planet formation scenarios. An interpretation of direct imaging surveys is also closely related to models of the dynamical relaxation (Veras, Crepp & Ford 2009). Hence, even apparently odd solutions (like the Trojan configurations), consistent with observations, should not be skipped a priori. Because the parent star may be very young (30 Myr or less), and the dynamical separation of planets in terms of the mutual Hill radii (Chatterjee et al. 2008), $K \sim 2$, the three-planet system is *strongly unstable* in a few hundred orbital periods time-scale (see their fig. 29; although these calculations are for more compact, Solar system like models and planets in Jupiter mass range). So the HR 8799 system might be not yet dynamically relaxed, remaining in a stage of planet-planet scattering. On the other hand, we may be ‘fooled’ by the significant errors of the initial condition implied by short time-base of the astrometry. Then the requirement of the dynamical stability may help us to find long-living systems close to apparently unstable best-fitting configurations.

As is well known, the phase space of a compact multiplanet system has non-continuous structure with respect to any notion of stability. The permitted region in the 18-dimensional parameter space of the HR 8799 system is large and has complex shape. To explore it efficiently, we apply a variation of the GAMP method (see e.g. Goździewski et al. 2008, for details) which relies on

Table 1. Osculating elements of the best-fitting solutions at the epoch of 2008 September 18. Formal errors of kinematic Fits I and II can be estimated graphically, see Fig. 1. Note that formal errors of dynamical GAMP Fits III and IV can be taken the same as for Fits I and II but the error ranges are strictly limited to stable regions of the phase space. The same concerns Fit V (see the text). The orbital inclination and nodal longitude (Fig. 1e) and arguments of pericentre (not shown here) are unconstrained. We set $i \in [0^\circ, 30^\circ]$, consistent with estimates of Marois et al. (2008), following the rotation model of the star.

Fit	Planet	$m (M_J)$	a (au)	e	ω ($^\circ$)	\mathcal{M}_0 ($^\circ$)	$m_0 (M_\odot)$	i ($^\circ$)	Ω ($^\circ$)	$(\chi^2_v)^{1/2}$
I	b	6.509	95.680	0.255	65.242	11.04				
Kinematic	c	12.57	52.364	0.269	335.95	0.740	1.200	19.8	68.3	1.55
Unstable	d	12.10	24.420	0.399	106.32	71.08				
II	b	6.108	90.676	0.212	289.28	1.480				
Kinematic	c	9.644	52.275	0.279	171.84	8.686	1.225	19.6	219.5	1.56
Unstable	d	7.806	49.855	0.587	9.0134	15.42				
III	b	8.022	68.448	0.008	308.59	191.7				
GAMP	c	11.87	39.646	0.012	353.83	40.03	1.445	15.5	11.12	1.88
Stable 1d:2c:4b MMR	d	8.891	24.181	0.075	144.38	127.6				
IV	b	9.708	67.661	0.014	29.671	123.8				
GAMP	c	7.963	31.045	0.248	243.41	158.8	1.611	11.4	357.2	2.03
Stable 1d:1c MMR	d	7.397	30.777	0.267	348.38	326.5				
V	b	8.325	73.543	0.043	122.49	357.8	1.448	17.9	30.9	1.48
GAMP (stable \sim 2c:5b MMR)	c	9.011	39.358	0.076	307.34	61.35				

self-adapting optimization based on the genetic algorithms (GAs; e.g. Charbonneau 1995; Deb, Anand & Joshi 2002) and on ‘penalizing’ unstable configurations by an appropriate term added to the mathematical value of $(\chi^2_v)^{1/2}$. Here, the penalty term is expressed through the diffusion of fundamental frequencies (Šidlichovský & Nesvorný 1996; Robutel & Laskar 2001).

An extensive GAMP search revealed long-term stable best-fitting III (Table 1) illustrated in Fig. 2(III). We note that its $(\chi^2_v)^{1/2} \sim 1.88$, remaining within 2σ range of the nominal, kinematic Fit I. To understand this solution, we computed the dynamical map in terms of the spectral number (SN), the fast indicator invented by Michtchenko & Ferraz-Mello (2001), and the max e (the maximal eccentricity attained during prescribed integration time). The SN map is illustrated in Fig. 3. Fit III lies inside a small island of regular motions (its width for the innermost planet is only ~ 0.3 au). A map of the max e indicator (not shown here) reveals that outside this region, one of orbits become highly eccentric that leads to catastrophic events during $\sim 10^6$ yr. Fit III describes a configuration involved in the Laplace-type three-body resonance, 1d:2c:4b MMR. Its critical argument is shown in the middle panel of Fig. 4. A similar solution was already found by Fabrycky & Murray-Clay (2008) and analysed in more detail by Reidemeister et al. (2009). Actually, our Fit III is also unstable but on a very long time-scale. After ~ 400 Myr, the innermost eccentricity suddenly grows and the Laplace resonance disrupts (see two upper panels in Fig. 4), indicating a collision. Hence, the small amplitude of the resonance angle does not protect the system from the collision. In fact, Fit III is formally chaotic that is indicated by the mean exponential growth of nearby orbits (MEGNO) in Fig. 4. This shows that the stability depends on long-term effects of the three-body mutual interactions and is tightly related to formally chaotic or regular character of tested configurations.

Besides Fit III, we also found a *stable* fit related to 1c:1d MMR, with moderate $e_{c,d} \sim 0.25$ and $a_{c,d} \sim 31$ au, see Figs 1 and 2(IV). Its $(\chi^2_v)^{1/2} \sim 2$ is still acceptably small because it lies within the formal 3σ level of the best Fit I. The dynamical SN map of this fit is shown in Fig. 5. It reveals also a small island of stable motions having the width comparable to Fit III. Simultaneously, planet b remains in a narrow island close to (1c:1d):3b MMR. The Trojans live at least over 3 Gyr – this system is close to quasi-periodic one, as indicated

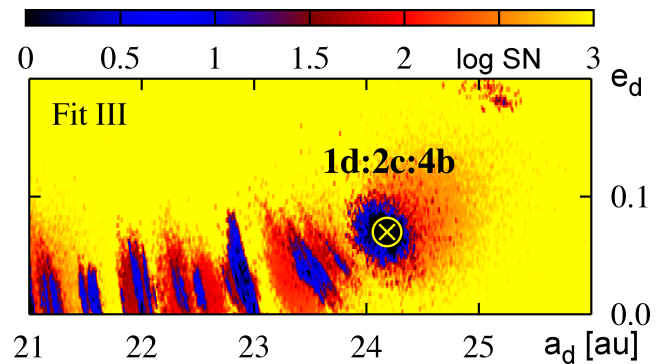


Figure 3. The SN map around stable Fit III (yellow rectangle in Fig. 1) in the (a_d, e_d) plane; other elements are fixed at their nominal values (see Table 1). Yellow colour is for strongly chaotic systems, black is for stable solutions. The maximal integration time for each pixel is 10 Myr ($\sim 25\,000 P_d$).

by $\langle Y \rangle(t) \sim 2$ (Cincotta, Giordano & Simó 2003) over large part of the integration time (Fig. 6). Still, a 10-Myr MEGNO map (not shown here) reveals that the island of regular solutions is very tiny (~ 0.01 au). Actually, this fit is also weakly chaotic although during first 600 Myr it appears as regular. This solution reveals peculiar small-amplitude librations of apsidal angle $\Delta\varpi(t) = \varpi_d - \varpi_c$ around 100° (the upper panel in Fig. 6). It might be the first case of *asymmetric* librations in the 1:1 MMR observed in a real system, and predicted already in low-order resonances (in particular, in 2:1 MMR; Hadjidemetriou 2006).

3 THE ASTRONOMICAL STABILITY OF THE SYSTEM

The phase space of the HR 8799 system appears strongly chaotic, with tiny islands of regular two- and three-body MMRs. Hence, to study its long-term (but finite) evolution, we might rely on a notion of the *astronomical stability* (Lecar et al. 2001), rather than on the formal Arnold’s stability analysed above. The astronomical stability may be investigated only by direct numerical integrations. Because the fate of chaotic configurations is hardly predictable, we attempted to gather statistics on initial conditions providing

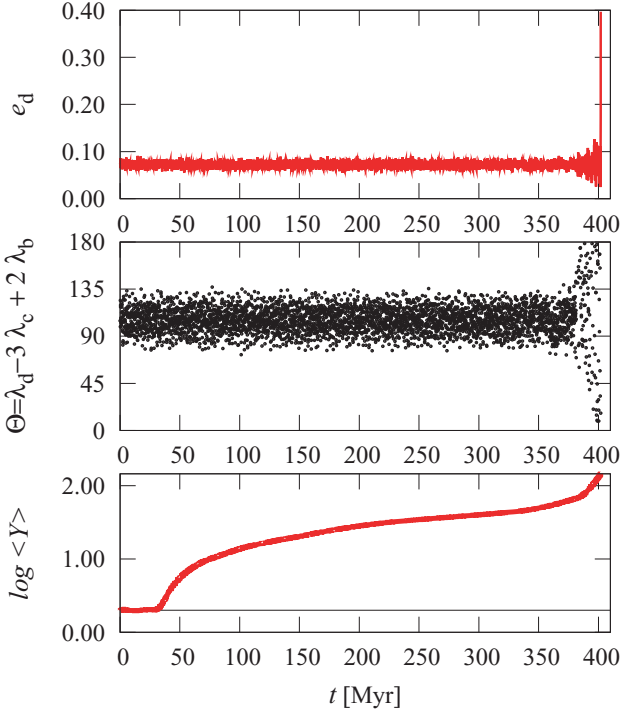


Figure 4. The innermost eccentricity in Fit III (the top panel), the argument of the Laplace resonance $\theta = \lambda_d - 3\lambda_c + 2\lambda_b$ (the middle panel) and MEGNO, $\langle Y \rangle(t)$ (the bottom panel). $\langle Y \rangle(t)$ converges to 2 for regular systems and diverges linearly for chaotic motions (Cincotta et al. 2003).

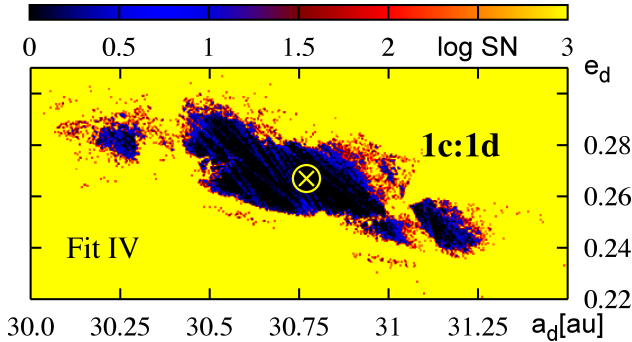


Figure 5. Dynamical SN map of a stable 1c:1d MMR (Fit IV, see Table 1).

long-living configurations, i.e. characterized by the *event time* T_E of a close encounter/ejection of a planet from an initial system.

We tested initial conditions within formal 3σ level of the nominal Fit I. To search for long-living systems, we again applied the GAMP algorithm, with the penalty term $\Delta(\chi_v^2)^{1/2}$ multiplied by $\tau = 1 - \|T_E/\Delta t\|$, where Δt is the maximal integration time relative to the initial (present) epoch $t = t_0$. In the first simulation, we integrated the system over $\Delta t = -30$ Myr (backwards), keeping track of solutions that survived as three-planet configurations. Next, the GAMP sample of ~ 2000 solutions ‘living in the past’ was integrated up to $\Delta t = +100$ Myr. The results are shown in Fig. 7. Fig. 7(a) is for the orbital periods ratio of systems that survived as three-planet configurations. It indicates that such systems are close to the 1d:2c MMR; the outer planets may be also involved in 1c:2b MMR or other low-order MMRs (like 2c:5b). That agrees well with the results of Fabrycky & Murray-Clay (2008). Moreover, most of the tested systems self-disrupted. Two remaining panels in Fig. 7

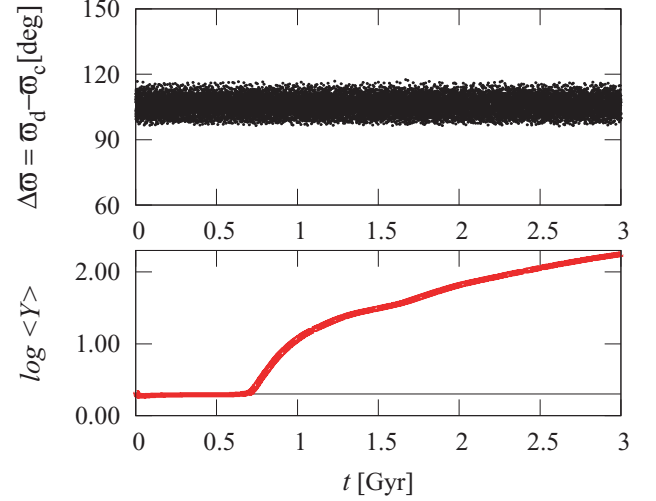


Figure 6. Long-term stability of the best-fitting solution with two inner planets involved in 1:1 MMR (Fit IV, see Table 1). The upper panel is for apsidal angle $\Delta\omega = \omega_d - \omega_c$. The bottom panel is for the MEGNO indicator.

are for the final osculating elements in the two-planet sample. Because of intensive planet–planet scattering (we recall that $K \sim 2$), the distribution spans large ranges of semimajor axes and almost whole available range of eccentricity. The strongly chaotic character of the HR 8799 system leads to rapid collisions/ejections in most of tested configurations during at most a few Myr. That confirms globally that the dynamical maps shown in Figs 3 and 5 represent a generic picture of the phase space, although they were computed for particular (resonant) initial conditions. Still, only ~ 400 systems of the total population, i.e. less than 20 per cent survived the integrations. In fact, the sample is ‘biased’ by the selection of systems surviving the integrations backwards. We found that direct Monte Carlo integrations leave much less than 1 per cent of astronomically stable configurations after 100 Myr. Hence, the self-adapting GAMP is crucial in this test because the direct Monte Carlo simulations would lead to unacceptable CPU overhead. Actually, there is no guarantee that systems astronomically stable in the 100-Myr test will also remain stable on longer time-scale, as shows the case of Fit III. In this experiment, we also found ~ 20 per cent of single-planet systems, and the rest in the sample ended as two-planet configurations. These dynamically relaxed two-planet systems appear highly hierarchical, with a strong maximum of semimajor axes ratio $\alpha \sim 0.05$ (see also Figs 7b and c).

4 TWO-PLANET HYPOTHESIS

Up to now, we assumed that the HR 8799 hosts *three* planets. Due to short observations that revealed planet d (a few weeks only), its orbit is unconstrained. Marois et al. (2008) claim a 6σ detection of the common proper motion, consistent with the Keplerian orbit. It is enforced by the absence of HR 8799d in the HST images in 1998 (Lafrenière et al. 2009) that otherwise should be seen in the subtracted light annulus (C. Marois, private communication). Still, we look here for an alternative explanation of the strongly unstable HR 8799 system due to projected brown dwarf or already ejected planet that would be really too distant to influence orbits of HR 8799b,c. We repeated the GAMP experiment for such two-planet model. We found easily rigorously stable solutions with $(\chi_v^2)^{1/2}$ comparable with the nominal, kinematic best-fitting system. Elements of the

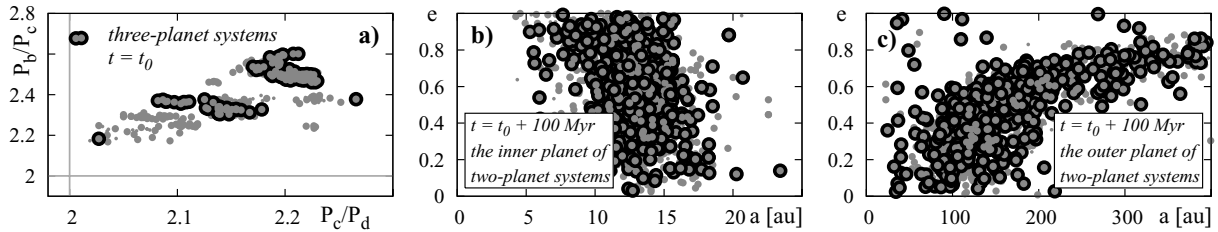


Figure 7. Osculating elements of configurations astronomically stable over $\Delta t = +100$ Myr after the initial epoch t_0 in terms of orbital periods ratio (panel a). Panels (b) and (c) illustrate the distribution in the (a, e) plane of the final, dynamically relaxed systems of two planets.

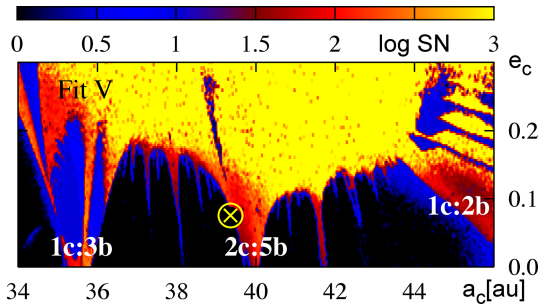


Figure 8. Dynamical (a_c, e_c) map of the best Fit V (see Table 1) of two-planet configuration in terms of the SN indicator. Its position is marked by a crossed circle. Most prominent structures of low-order MMRs are labelled.

best-fitting solution are given in Table 1 (Fit V). The two-planet fits within 1σ bound span a wide range of semimajor axes ~ 10 au and may be stable up to $e_{b,c} \sim 0.15$. Their orbits are initially close to anti-aligned. Planetary masses in such systems remain in the $10 M_J$ range, which is well consistent with astrophysical constraints given in Marois et al. (2008); we note that stable three-body fits tend to much lower masses than declared (Fabrycky & Murray-Clay 2008). Furthermore, the dynamical map in Fig. 8 reveals extended zones of stability and a proximity of the best-fitting solution to the 5:2 MMR, recalling the Jupiter–Saturn pair in the Solar system.

5 CONCLUSIONS

The dynamical analysis of available astrometric data of HR 8799 reveals that its massive companions are involved in heavy mutual interactions. Assuming 1σ range of the planetary and star mass astrophysical estimates, the search for stable (regular) systems brings only narrow and very limited islands of ordered motions. Most likely, the system can be long-term stable if is involved in low-order two- or three-body MMRs (particularly, in the Laplace 1d:2c:4b MMR). Here, we confirm the results of Fabrycky & Murray-Clay (2008) and Reidemeister et al. (2009), which we derived after independent, quasi-global GAMP calculations. Moreover, also peculiar 1d:1c MMR Trojan systems stable over a few Gyr can be found.

The outstanding discovery, in the light of the dynamical analysis, brings a few open questions. How the three-planet system may be captured in such tiny regions of stable motions? Are in fact planetary masses much lower than estimated? Or is the system substantially non-coplanar? Both factors could extend the zones of stability. While the masses may be constrained by astrophysical factors and astrophysical-age estimates (Marois et al. 2008; Reidemeister et al. 2009), we can say little on the real mutual inclinations. Further, if we skip the less constrained object, the sub-system of two outermost objects remains stable, resembling the Jupiter–Saturn pair,

even if the masses are large, apparently solving the puzzle. It may be verified soon, thanks to the shortest orbital period of planet d.

Actually, should we expect that the system is or must be stable? Its parent star is very young, and we may have an opportunity to observe a system undergoing the dynamical relaxation. The statistical analysis suggests that the final fate of coplanar systems constrained by available astrometric data most likely will be two-planet, highly hierarchical configuration with eccentric orbits. Our calculations show that less than 20 per cent of systems stable in the past and remaining in the neighbourhood of the best stable Fit III remain stable after 100 Myr. Likely, even much less number of configurations survives longer time due to possible, chaotic effects of the three-body interactions (MMRs overlapping; Murray & Holman 2001). A conclusion of Fabrycky & Murray-Clay (2008) may be repeated here. Although HR 8799 has been directly imaged, the interpretation of its images is very difficult and yet non-unique. Longer observations are required to constrain orbits of its planets.

ACKNOWLEDGMENTS

We warmly thank Daniel Fabrycky for an informative review that greatly improved the manuscript. Many thanks to Christian Marois for corrections and permission to use images of HR ~ 8799 , and to Alexander Krivov and Ralph Neuhäuser for a discussion. This work is supported by the Polish Ministry of Science, through Grants 1P03D 021 29 and 92/N-ASTROSIM/2008/0.

REFERENCES

- Charbonneau P., 1995, *ApJS*, 101, 309
- Chatterjee S., Ford E. B., Matsumura S., Rasio F. A., 2008, *ApJ*, 686, 580
- Cincotta P. M., Giordano C. M., Simó C., 2003, *Physica D*, 182, 151
- Deb K., Anand A., Joshi D., 2002, *Evol. Comput.*, 10, 371
- Fabrycky D. C., Murray-Clay R. A., 2008, *ApJ*, submitted (arXiv:0812.0011)
- Fukagawa M. et al., 2009, *ApJ*, 696, L1
- Goździewski K., Migaszewski C., Musielniński A., 2008, *Proc. IAU Symp.* 249, 447
- Hadjidemetriou J. D., 2006, *Celest. Mech. Dyn. Astron.*, 95, 225
- Jurić M., Tremaine S., 2008, *ApJ*, 686, 603
- Lafrenière D., Marois C., Doyon R., Barman T., 2009, *ApJ*, 694, L148
- Lecar M., Franklin F. A., Holman M. J., Murray N. J., 2001, *ARA&A*, 39, 581
- Marois C. et al., 2008, *Sci*, 322, 1348
- Michtchenko T. A., Ferraz-Mello S., 2001, *AJ*, 122, 474
- Murray N., Holman M., 2001, *Nat.* 410, 773
- Reidemeister M. et al., 2009, *A&A*, submitted
- Robutel P., Laskar J., 2001, *Icarus*, 152, 4
- Scharf C., Menou K., 2009, *ApJ*, 693, L113
- Šidlichovský M., Nesvorný D., 1996, *Celest. Mech. Dyn. Astron.*, 65, 137
- Veras D., Crepp J. R., Ford E. B., 2009, *ApJ*, 696, 1600

This paper has been typeset from a $\text{\TeX}/\text{\LaTeX}$ file prepared by the author.